The Thesis Committee for Gabriela Idania Vargas-Zúñiga
Certifies that this is the approved version of the following thesis:

π-Metal Complexes of *i*-Propyldinaphthoporphycene

APPROVED BY
SUPERVISING COMMITTEE:

Supervisor:

Jonathan L. Sessler

Christopher Bielawski

π-Metal Complexes of *i*-Propyldinaphthoporphycene

by

Gabriela Idania Vargas-Zúñiga, B.S. M.S.

Thesis

Presented to the Faculty of the Graduate School of

The University of Texas at Austin

in Partial Fulfillment

of the Requirements

for the Degree of

Master of Arts

The University of Texas at Austin

August, 2011

Acknowledgements

I would like to thank my advisor Prof. Dr. Jonathan L. Sessler, for his constant belief in my abilities and support, and for encourage me to learn more and always give my best no matter the adversities or limitations.

Thank you very much to every single Sessler group member, for the good time I have had in the lab.

Sung Kuk, you have been a great labmate, who has taught me everything I know. I appreciate a lot all the good words that you always have for me. All the help that you have given to me related to chemistry has been of a great value for me.

Christian, Christopher, Elizabeth, and Vladimir thank you very much for your friendship.

I would also like to express my gratitude to my family for their constant support and love.

Abstract

π-Metal Complexes of *i*-Propyldinaphthoporphycene

Gabriela Idania Vargas-Zúñiga, M.A.

The University of Texas at Austin, 2011

Supervisor: Jonathan L. Sessler

Porphycenes have attracted attention for their ability to stabilize complexes with a wide range of metal cations. Coordination compounds of these macrocycles are endowed with of specific chemical, optical, electronic, spectroscopic and photochemical properties,[1-8] such as, strong absoptions in the red region of the UV-vis spectrum. These characteristics have been used in the study of protein mimicry,[9, 10] photodynamic therapy (PDT)[11-16] and materials chemistry[17, 18] The fusion of bipyrrolic entities with aromatic rings could led to a change in the photophysical properties of porphycenes, and could give rise to nonlinear optical (NLO) behavior.[19] Taken in concert, these possibilities provides an incentive to study metal complexes of new porphycenes. With that goal in mind, presented here is the synthesis and the spectroscopic and voltamperometric analyses of four metollocene complexes of a relatively new annulated porphycenes, namely *i*-propyldinaphthoporphycene.

Chapter 1 of this thesis provides a brief introduction into porphycenes and porphyrins as well as complexes prepared from these macrocycles. Because it relates more closely to the research described in this thesis, the emphasis will be on peripherally substituted and directly π-metallated porphyrin-like macrocycles.

Annulated porphycenes and their metal complexes display geometric and optical features that differ from those of normal porphycenes. Chapter 2 details the coordination compounds of annulated porphycenes, as well as some of their optical and redox features. This chapter also summarizes the current synthesis of dinaphthoporphycenes, while detailing efforts by other authors to coordinate transition metals to dinaphthoporphycenes, which culminated in the preparation of the first nickel(II) complex known so far with this ligand.

It was recently found that the electronic properties of porphycenes change from those of an electron donor to those of an electron acceptor when the RuCp* (Cp*: pentamethylcyclopentadienyl) fragment is coordinated to the "π-face" of the macrocycle. This finding, discovered using so-called etioporphycenes, motivated the author to explore the metal complexation chemistry of *i*-porpyldinaphthoporphycene. This led to the synthesis of four metalloporphycenes are described in Chapter 3. Here, the coordination of the $[M(Cp^*)]^{n+}$ (M = Ru, Ir and Rh) fragments to the π-electron framework was established by analytical, and structural means. Thus, this chapter provides of a description of the spectroscopic, structural and voltamperometric features of these complexes.

Table of Contents

List of Figures

List of Schemes

List of Tables

Chapter 1: π-Metallated Porphyrin-like Complexes

1.1. Porphycenes – Constitutional Isomers of Porphyrins

Porphyrins have been recognized as distinct chemical entities for over a century.[10, 11] This basic structure and the associated chemical features were elucidated by Hans Fischer in the early 20th century, work for which he was awarded the Nobel Prize in 1930. Since then, these tetrapyrrolic aromatic macrocycles have been widely studied by chemists. Inspiration for this effort comes from their role in biological processes, such as photosynthesis and respiration. In order to study the correlation between structure and function in greater detail, researchers have focused on in the preparation of new prophyrin analogues, such as the porphycenes (Figure 1.1). Porphycene, formally known as [18]porphyrin-(2.0.2.0), is a constitutional isomer of porphyrin that was first prepared in 1986 by Vogel and coworkers.[12] These macrocycles contain two 2,2'-bipyrrole subunits linked by two double bonds to form a tetraaza central core.[13] This structural characteristic make the porphycenes less symmetric than similar substituted porphyrins. It also engenders different optical properties, such as strong absorption features in the red region of the UV-Vis spectrum (e.g., strong absorption between 620 to 760 nm). These features have made porphycenes of interests in various biomedical applications, including photodynamic therapy (PDT) and the photoinactivation of viruses and bacteria, particularly in the area of blood purification.[14]

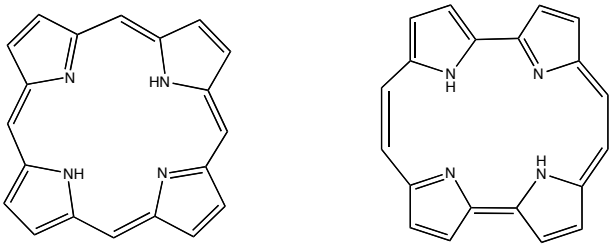

Figure 1.1: Basic structures of porphyrin and porphycene.

Since the synthesis of the first porphycene was published, several porphycene derivatives have been reported.[12-15] In analogy to what is true for porphyrins, the capacity for metal cations coordination and the basic requisite optical properties of porphycenes can be modified by the attachement of substituents. The functionalization may be achieved on the β-pyrrolic positions, to give so-called etioporphycenes. Or, it can be achieved the ethynyl brindges or at the *meso* positions (Figure 1.2). Other types of functionalization include, 1) the use of fused aromatic rings on the pyrroles, which produces, e.g., tetrabenzoporphycenes, and 2) linkages between two adjacent pyrrolic rings, which produce, e.g., benzoporphycenes, as will be detailed in the next chapter.[14]

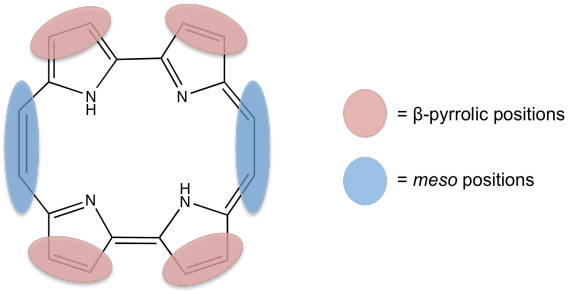

Figure 1.2: Porphycene framework.

1.2. Metal Complexes of Porhycenes

Given their close structural similarity to porphyrins, porphycenes also form metal complexes with transition metals. However, in comparison to those of the porphyrins, the electrochemical behavior upon electroreduction of metalloporphycenes is different. For instance, the metal complexes of octaethylporphycene, **1**, display a smaller HUMO-LUMO gap (1.85 ± 0.5 V), than the related complexes with octaethylporphyrin, **2**, (2.25 ± 0.15 V). This behavior is attributed to the fact that porphycenes differ structurally from porphyrins. As noted above, these differences include the presence of a smaller cavity and a lower level of symmetry (D_{2h} for **1** and D_{4h} for **2**).[15]

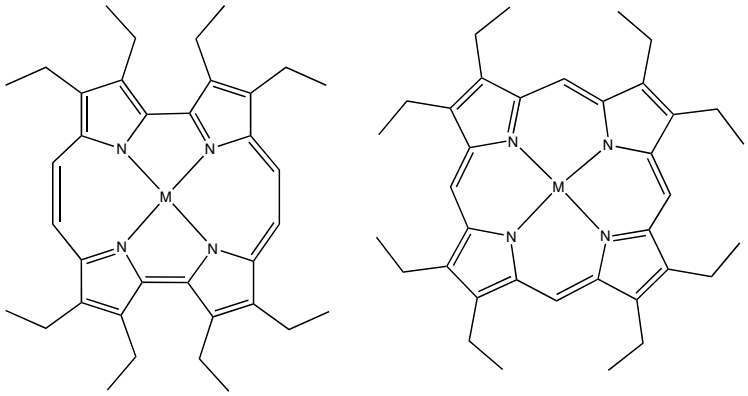

1 2

M= Mn, Fe, Co, Ni,Cu, Zn

Although possessing a smaller cavity, metal complexes with larger metal cations, such as ruthenium and osmium, have been obtained in the case of porphycene (Scheme 1). Coordination of the relatively large osmium and ruthenium ions was achieved by the reaction of 2,7,12,17-tetrapropylporphycene (H_2TPrPc) with triruthenium or triosmium dodecarbonyl, [$M_3(CO)_{12}$] (M= Ru, Os). This gave carbonylruthenium(II) porphycene, **3**, and carbonylosmium(II) porphycene, **4**.[16] Compared to the analogous porphyrin complexes with osmium and ruthenium, the porphycene complexes displayed similar optical properties. The insertion of these large metals into the small porphycene is thought possible due to a reduction in the metal size resulting from back-bonding with the carbonyl ligands.[17-19] Interestingly, the oxidation of **4** resulted in the generation of the corresponding dioxoosmium(VI) porphycene complex, **5**, a species that resembles the corresponding porphyrin system.

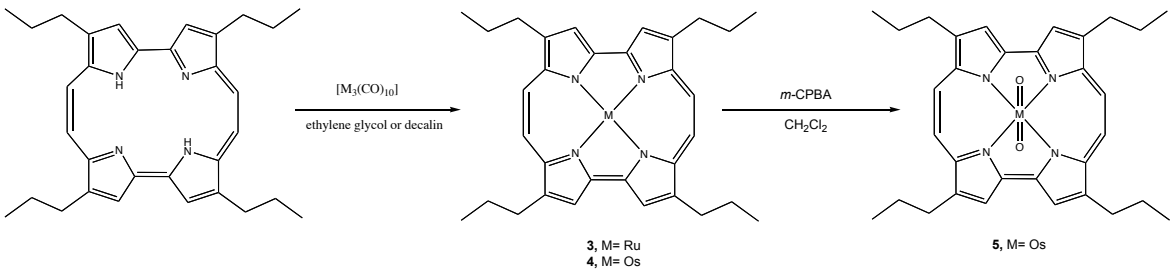

Scheme 1.1: Synthesis of carbonylruthenium(II) porphycene complex, **3**, carbonylosmium(II) porphycene complex, **4**, and dioxoosmium(VI) porphycene complex, **5**.[17-19]

1.3 π-Metallated Porphyrin Complexes

Most of the coordination chemistry involving porphyrin-like macrocycles has been focused on complexes stabilized by σ-type interactions between the bound cations and the nitrogens of the pyrroles. Less common is π-coordination of a metal center either to a peripherial substituent or directly to one or more pyrrole subunits. This type of coordination has been explored as a possible way to modify the electronic and optical properties of the macrocycle. Over the last few decades, π-metallated porphyrins have been reported. The first example was the π-coordinated complexes **6** and **7** reported by Gogan and Siddiqui in 1970.[20, 21] Complexes **6** and **7** involve substitution on a porphyrin pyrrole. They were obtained by reacting $[Cr(CO)_6]$ with either tetraphenylporphyrin or the corresponding metallotetraphenylporphyrin under a nitrogen atmosphere. Under these conditions, only the tricarbonyl chromium π-complexes of the [ZnTPP] and the metal-free chromium π-complex were isolated. Further studies revealed that there was no communication between the peripheral metallic fragment and the macrocycle, a finding that was attributed to an unfavorable conformational arrangement (Figure 1.3).

Other examples of peripherally π-coordination involving metalloporphyrin systems were reported by Smith, Kadish and coworkers.[22, 23] In this case, the products, the monoruthenocene porphyrin **8** and the bisporphyrinatoferrocene **9** derivatives (see Figure

1.3), were synthetized by reacting [Cp*$RuCl_2$] (Cp* = pentamethylcyclopentadienyl) or $FeCl_2$ with porphyrin as a free ligand. The crystal structure of complex **8** revealed that a ruthenocene was bound to the fused cyclopentadyene ring of the macrocycle, while compound **9** consisted of two porphyrin macrocycles connected by a ferrocene moiety. An X-ray diffraction analysis of **9** revealed that the ferrocene fragments were essentially eclipsed and that the zinc(II) two constituent porphyrin subunits were not parallel. In both complexes, **8** and **9**, UV-vis and electrochemical studies led to the conclusion that there was an electronic interaction between the metallocene and the metalloporphyrin molecules. However, attempts to obtain other stable π-metallated porphyrin derivatives failed, presumably as a consequence of the unstable nature of the products obtained.

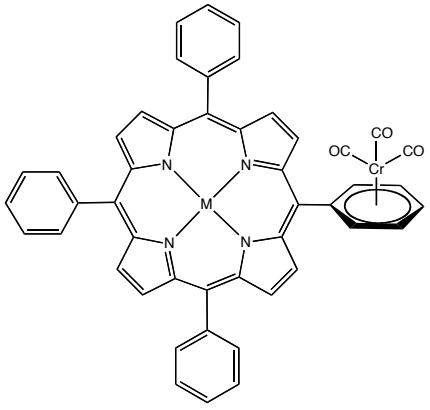

M = Cr, MnCl, Co, Ni, Zn

6

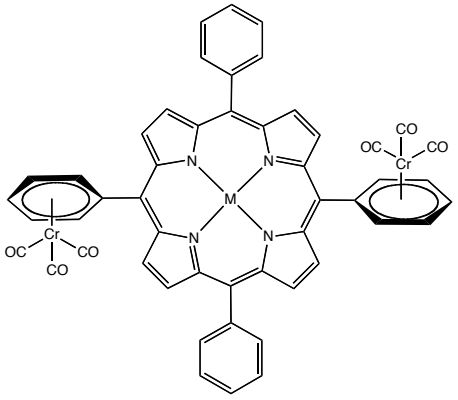

7

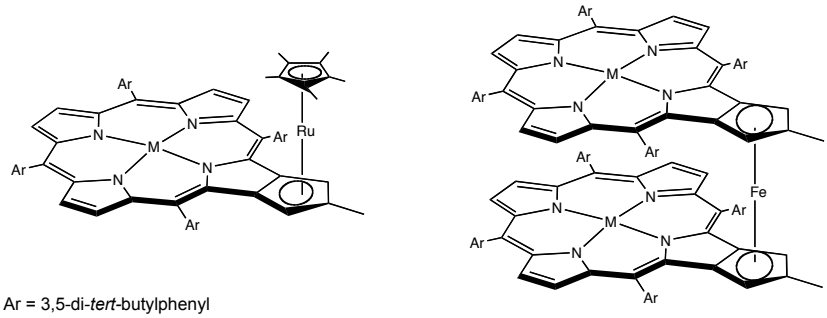

Ar = 3,5-di-*tert*-butylphenyl

M = Cu, Ni, Zn

8

M = Ni, Cu, Zn

9

Figure 1.3: Examples of peripherally π-metallated porphyrins prepared by Gogan and Siddiqui (**6** and **7**),[20, 21] and Smith and Kadish (**8** and **9**).[22, 23]

The first directly π-metallated porphyrins were reported by Rauchfuss *et al*. in the middle 1990s.[24, 25] In this case, an X-ray diffraction analysis of the complex involved, **10**, revealed that the porphyrin ligand was distorted from planarity. However, the organometallic fragment was found to lie almost parallel to the macrocycle. The metalloporphyrin thus acts as a ligand, but was able to coordinate only one metallocene (Figure 1.4). The UV-vis spectra revealed a bathochromic shift, as well as a quenching of the fluorescence. The findings were taken as evidence that π-complexation of a metallocene changes the electro- and photochemical properties of the metalloprophyrin from which the complex derives. Subsequently, Sessler, Kadish and Fukuzumi, studied the electronic communication between the metal centers within a set of π-coordinated porphyrin complexes.[26, 27] The octaethylporphyrin-ruthenocene complexes, **11**, used for these studies were characterized by a planar conformation. The UV-vis and fluorescence spectra of these complexes displayed a broadened, red-shifted and very weak fluorescence. These findings were taken to indicate that coordination of the π-bound ruthenocene moiety caused a strong electronic perturbation as the result of an effective electronic communication between the ruthenocene and the macrocycle. Further insight

into the coupling within these systems showed came from laser flash photolysis analysis. Here, it was found that the photoirradiation induced an electron transfer from the ruthenocene moiety to the singlet excited state of the metalloporphyrin. This finding provided support for the notion that this porphyrin, and presumably others could be modified by electronic properties of porphyrins fusion of a metallocene to the porphyrin core. Specifically, these results underscore the suggestion that porphyrins could be switched in this way from being an electron donor to being an electron acceptor.[26, 27]

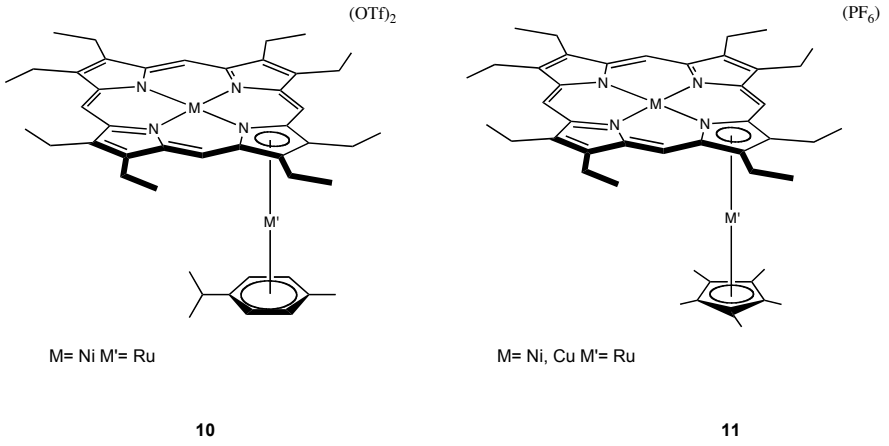

Figure 1.4: Examples of directly π-metallated porphyrins, which involve the pyrrolide subunit of a metalloporphyrin acting as a ligand.

1.4 π-Metallated Porphycene Complexes

As has been detailed earlier on in this chapter, direct coordination of a $[RuCp^*]^+$ fragment to the π-electron face of octaethylporphyrin changes the electronic properties of the macrocycle. This modulation, observed *via* a photoinduced electron transfer from the ruthenocene moiety to the porphyrin,[26] provided a motivation to extend these fundamental studies into the realm of porphycenes. While σ-metal coordination of porphycenes has been widely studied by several groups, the corresponding π-coordination chemistry was unknown until recently. In fact, it was only several years ago

that Sessler and collaborators reported the first synthesis of bimetallic complexes (e.g., **12**) with porphycenes involving π-coordination.[27, 28] The complexes in question consisted of a $[Ru(Cp^*)]^+$ fragment coordinated the π-electron "face" to an allyl substitution porphycene. Either Ni(II) or Cu(II) cations were σ-coordinated to the central N_4 core, as shown in structure **12** of Figure 1.5. An X-ray diffraction analysis of several of these complexes revealed a planar macrocycle conformation, with the Cp* fragment being oriented parallel to the macrocycle.

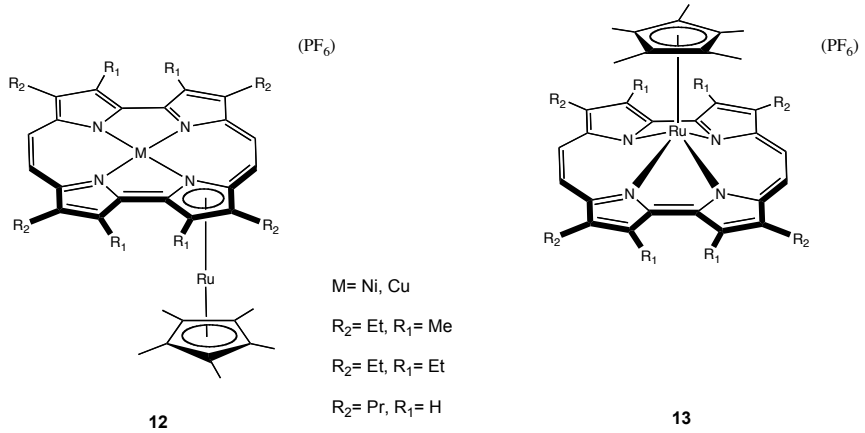

Figure 1.5: π-Complexes of metalloporphycenes **12** and "sitting atop" semi-sandwich complexes **13**.[28]

Spectroscopic and electrochemical studies of these complexes revealed evidence for a strong interaction between the macrocycle and the oragnometallic fragment. The UV-Vis spectra of these bimetallic complexes revealed that the Q-band is red-shifted (to around 870 nm), which is consistent with an effective electronic communication between the organometallic fragment and the porphycene core. Photophysical studies of type **13** complexes revealed that fusion of the ruthenocene moiety to the porphycene core allowed for a photoinduced electron transfer from the metal center to the porphycene core upon photoexcitation. This observation was taken as evidence that, in analogy to what was seen for the corresponding metalloporphyrin complexes of this type, coordination of this

particular organometallic fragment to the π-electron face of the pyrrole serves to change the porphycene from an electron donor to an electron acceptor.

Efforts by Sessler and collaborators to coordinate a $[Ru(Cp^*)]^+$ fragment to metal-free porphycenes failed. Instead, so-called "sitting atop" semi-sandwich complexes, such as **13,** were obtained. These complexes proved to possess different optical and electrochemical characteristics from the hybrid bimetallic porphycenes of type **12**. Firstly, the associated crystal structures revealed that the coordinated ruthenocene center lies out the N_4 porphycene plane and that the pyrrolide units of the porphycene macrocycle are tilted. Distortion of the η^5-Cp* ligand also results. Presumably, this is a consequence of the steric congestion between the β-substituent and the Cp* ring (see Figure 1.5). The electrochemical behavior of these complexes revealed that the Ru(IV) cation is not reduced. Rather a π-radical anion is formed, which allows an overall charge balance to be mantained. It was further inferred that the β-pyrrolic substituents influence the electronic characteristics of the "sitting-atop" complexes. For instance, the presence of four alkyl groups on the prophycene periphery provided a complex with a greater electron donor character than metalloporphyrins with eight alkyl groups. This led to the conclusion that the intramolecular electron transfer process can be modulated by the choice of the substituents present on the β-pyrrolic positions.[27, 28]

Chapter 2: Dinaphthoporphycenes

2.1 π-Expanded Porphyrins – A Brief Introduction to Annulated Porphyrins

Porphyrin derivatives that possess extended conjugation pathway have been of interest to researchers in recent years due in part to a red-shift in their light-absorbing features. Efforts to obtain red-shifted absorbing materials have led to the synthesis of systems with larger cores than natural porphyrins.[29, 30] However, the syntheses of these "expanded" porphyrins are often complicated and plagued by low yields. Another approach has been the development of π-extended porphyrin derivatives. These macrocycles incorporate additional aromatic rings on the periphery of the macrocyclic core. Examples of these annulated porphyrins are the tetrabenzo-, tetranaphtho-, and tetraanthroporphyrins, shown as structures **14**, **15** and **16** in Figure 2.1.[31] These modifications produce bathochromic shifts of the lowest-energy Q-band. For instance, the zinc complex of 5,10,15,20-tetraphenylporphyrin exhibits a λ_{max} for the lowest-energy Q-band of 602 nm in dichloromethane, while the zinc complex of the linearly annulated porphyrin, **15**, in the same solvent moves to 731 nm.

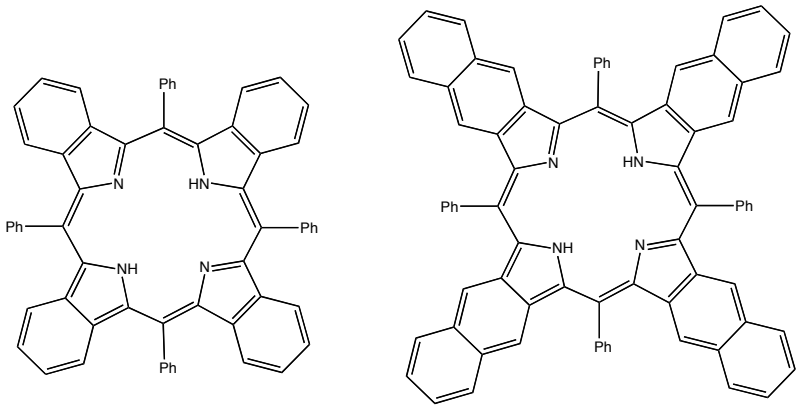

Figure 2.1: Examples of linearly annulated porphyrins.[31]

2.2 EXPANDED PORPHYCENES

As was mentioned above, the study of π-extended porphyrins has attracted considerable interest in recent years. However, few annulated porphycenes are known, and their optical and coordination features have been studied even less extensively. Tetra-*tert*-butyldibenzoporphycene, **14**, for instance, a π-expanded porphycene first reported by Vogel, [32-34] differs markedly in its geometrical and optical properties as compared to normal porphycene. Unlike non-annulated porphycenes, which are nonplanar and not particularly rigid, the annulated system **17** is characterized by a planar structure. One

consequence is an apparent reduction in the steric repulsions between the *t*-butyl groups and the adjacent ring hydrogen atoms. Presumably, as a result of this geometrical change, **17** no longer displays a pronounced Soret band. Likewise, it exhibits little in the way fluorescence emission intensity even at liquid nitrogen temperature (77 K).[33] This stands in contrast to nonplanar porphycenes.

Another annulated porphycene that has been reported is tetrabenzoporphycene, **18**.[35] This porphycene is characterized by a Q-band that is red-shifted relative to normal porphycenes. Presumably, this is the result of the π-extended framework; however, unlike tetra-*tert*-butyldibenzoporphycene, **18** exhibits a Soret band that has a high extinction coefficient. This contrast is thought to reflect the nonplanarity, nonrigidity, and lack of symmetry inherent in **18**. This macrocycle also proved capable of coordinating the nickel(II) cation.

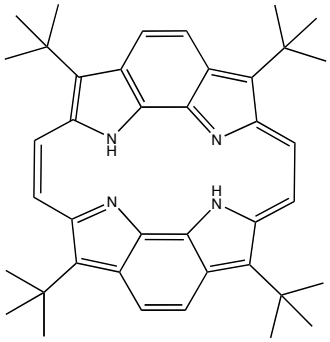

17

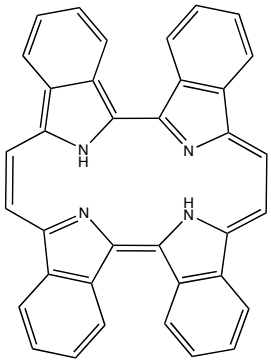

18

Recently, Sessler *et al*., and subsequently Panda and coworkers, published a new class of annulated porphycenes, called dinaphthoporphycenes, **19**-**21**.[29, 36] As true for the examples mentioned above, these planar systems were found to display absorption spectra that were bathochromically shifted as a result of an increase in the π-electron periphery. Similar to dibenzoporphycenes, the dinaphthoporphycenes **19** and **20** are not fluorescent. Again, this is ascribed to the rigidity of the frameworks involved. However, cyclic voltammetry studies of **20** revealed that this macrocycle is more susceptible to

oxidation than its nonannulated tetrapropyl porphycene parent, a finding ascribed to its π-extended structure (peak potentials at 0.89 and 1.24 V in dichloromethane). X-ray analysis of **20** revealed a nearly planar structure from which strong N – H – N bond interactions were inferred. Shortly after the Sessler report, Panda *et al*.[26] reported the nickel(II) complex with several dinaphthoporphycenes, such as **21** in Figure 2.2. This complex was obtained by heating the free base macrocycle at reflux in the presence of an excess of $Ni(acac)_2$. The absorption spectrum of these complexes displayed a red-shifted Soret bands and blue-shifted Q-bands. An X-Ray diffraction analysis of **21** revealed that the insertion of the metal cation in the macrocycle cavity confers a more planar conformation.

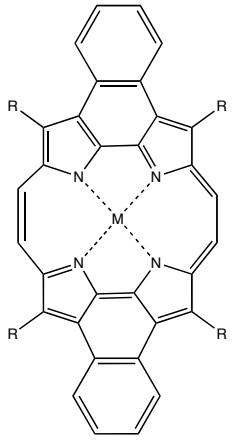

19, R = 1-ethyl-pentyl; M = 2H
20, R = *i*-Pr; M =2 H
21, R = *i*-Pr; M =Ni

Figure 2.2: Dinaphthoporphycenes **19** and **20**, and the *i*-propyldinaphthoporphycene nickel(II) complex **21**.[36]

Chapter 3: Synthesis and Characterization of π-Metal Complexes of *i*-Propyldinaphthoporphycene

As described in Chapter 1, a number of porphycenes and their metal complexes have been synthesized since Vogel *et al*. published their seminal report on the synthesis of porphycene in 1986.[12] However, metalloporphycenes that present a direct "fusion" of a metallocene complex onto the porphycene π-electron framework were unknown until the first ruthenocene bimetallic with nickel(II) and copper(II), and "sitting-a-top" semi-sandwich complexes with etioporphycenes were reported by Sessler and coworkers in 2009.[28] Separate from this, Sessler reported recently a new class of dinaphthoporphycenes, as well as a description of their optical features and electrochemical behavior (cf. Chapter 2). In addition, Panda *et al*. reported shortly thereafter the corresponding nickel(II) complexes of the same macrocycles. As yet efforts to study the π-coordination of metallocene fragments in these new porphycenes have not been made. The goal of this work was to explore the interaction of metallocenes with the metal-free form of *i*-propyldinaphthoporphycene, **20**. Described here is the formation of both mono- and bimetallic complexes (e.g., **24**-**26** and **27**, respectively, Scheme 3.2) formed through π-complexation. These systems, in which metallation takes place on the naphthalene subunit, appear to be the first examples of metalloporphycenes where the metallocene coordinates to the π-electron face of the prophycene leaving the N_4 core free. Characterization of these complexes was carried out *via* proton and carbon NMR spectroscopy, mass spectrometry and elemental analysis. X-ray structures of two complexes were also solved by Dr. Vincent Lynch from single crystals provided by the author.

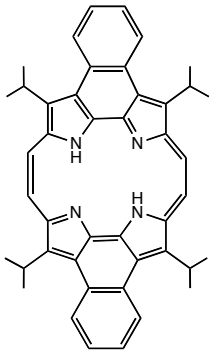

20

3.1 Synthesis and Crystal Structures

The naphthoporphycene used for these studies was prepared from bipyrrole **22** (provided by Vladimir Roznyatoskiy). Subjecting this precursor to Vilsmeier-Haack formylation gave **23** in a quantitative yield. Intramolecular McMurry coupling then produced the *i*-propyldinaphthoporphycene, **20** as reported in the literature.[12, 14, 29] Oxidation of the intermediate porphycenogen (produced as the initial product of the coupling) was carried out by exposing the yellow-green fluorescent solution obtained immediately after the McMurry coupling to air for 3 hours, Scheme 3.1 (instead of using DDQ as was reported). A chromatographic purification over silica gel or neutral alumina of the resultant black solution yielded the desired dinaphthoporphycene **20** in yields around 17%.

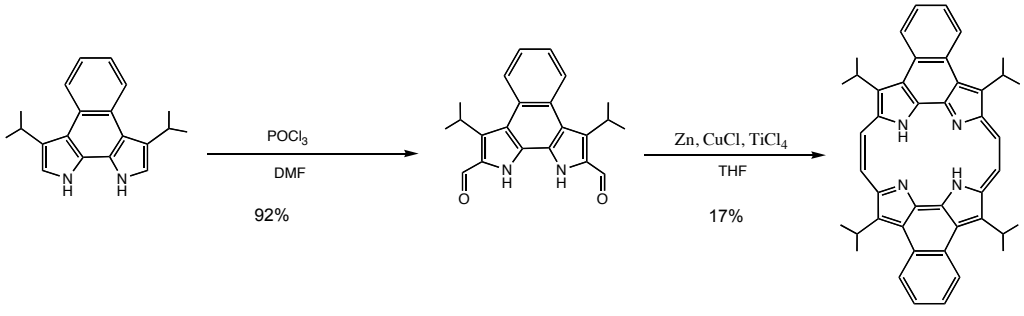

22 **23** **20**

Scheme 3.1: Synthesis of *i*-propyldinaphthoporphycene, **20**.

The metal complexes of **20** reported here were obtained by the reacting the metallocene salt with the free-base porphycene in a nonccoordinating solvent, such as dichloromethane or 1,2-dichloroethane. This afforded the sandwich complexes **24**, **25**, and **26** as dark green solids in roughly 40% yield. In these complexes, the metallocene fragment is π-coordinated to the naphthalene moiety, while the N_4 core remains free. (cf. Scheme 3.2). The bimetallic complex **27**, was synthesized from the nickel(II) complex, **21**.[36] Complex **27** was obtained from **21** by exposure to $[RuCp^*(NCMe)_3]PF_6$. The new compounds were isolated in moderate yields after chromatographic purification as air-stable solids and characterized by NMR (^1H and ^{13}C) spectroscopy, high resolution mass spectrometry and elemental analysis. Complexes **26** and **27** were also characterized by single crystal X-ray diffraction analysis.

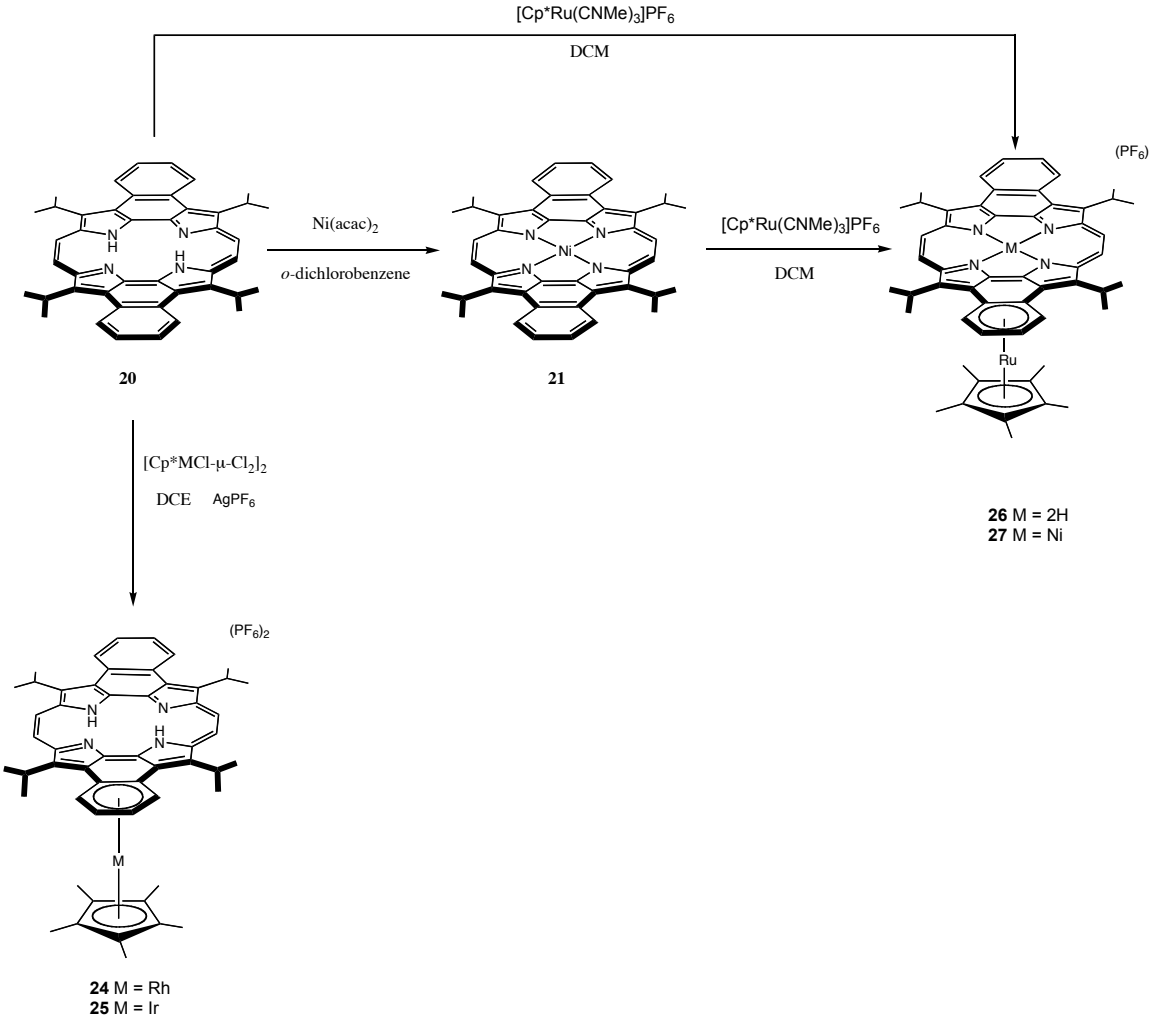

Scheme 3.2: Synthesis of metallocene *i*-propyldinaphthoporphycene π-complexes, **24**, **25**, and **26**, and the hybrid ruthenocene *i*-propyldinaphthoporphycene complex, **27**.

The attachment of a metallocene to the naphthalene moiety of the porphycene produces a loss of symmetry, which is reflected in the corresponding NMR spectra. For instance, the ^{1}HNMR spectra of complexes **24** and **25** revealed a set of nonequivalent of resonances corresponding to the naphthalene, *meso* protons and *i*-propyl substituents that

were shifted to lower field as compared to **20.** This finding is consistent with the proposed structure, specifically the conclusion that only one metallocene is able to coordinate to the π-electron face of the porphycene. The corresponding signal of the Cp* methyl groups was also shifted to higher field in these complexes. This observation is rationalized in terms of a strong interaction between the porphycene ring and the Cp* ligand.

Single crystals of complexes **26** (dark blue prisms) and **27** (very dark, almost black prims) suitable for single crystal X-ray diffraction analysis were obtained by slow evaporation from CH_2Cl_2 / diethyl ether and slow evaporation from dichloromethane, respectively. The resulting structures solved by Dr. Vinvent M. Lynch of this department are presented and discussed in Figure 3.1. The crystal structure of **26** revealed the $[Ru(Cp^*)]^+$ fragment π-coordinated to one of the naphthalene moieties and with the Cp* ligand in a parallel plane. The porphycene core is distorted from planarity with the pyrrolide units displaced upwards so as to accommodate the metallocene subunit. The average deviation of the nitrogen atoms from the main porphycene plane (excluding the isopropyl and ruthenocene substituents) is ± 0.11 Å. Unlike the ruthenocene-porphycene complexes reported previously by our group,[28] in **26** the N_4 core remains metal-free. Further, in contrast to what was observed in analogous complexes prepared from etioporphycenes (a class of octaalkyl substituted poprhycenes), a "sitting atop" complex involving the ruthenocene was not observed with dinaphthoporphycene under the experimental conditions employed. Similar N – N distance of 2.50 Å are seen in **26** and in the starting naphthoporphycene **20**.[29]

The crystal structure of **27** revealed the ruthenocene as being "fused" to the naphthalene fragment (see Figure 3.1). In this complex the nickel atom is coordinated within the N_4 core. However, it resides 0.18 Å out of plane. The N – N distances between the two pyrrolic nitrogens are 2.67 Å and 2.64 Å. These values are similar with what was reported by Panda *et al*. for the Ni-porphycene complex.[36] In analogy to what is seen for ruthenocene complex **26** lacking a central metal cation, distortion from planarity is seen for complex **27** at the level of the core naphthoporphycene subunit. Presumably, this is

the result of steric congestion between the *i*-propyl groups and the Cp* methyl groups. The average deviation of the central four nitrogen atoms from the main porphycene plane (excluding the isopropyl substituents and ruthenocene subunit) is ± 0.12 Å.

a)

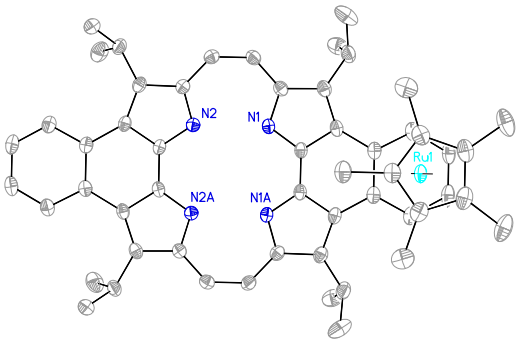

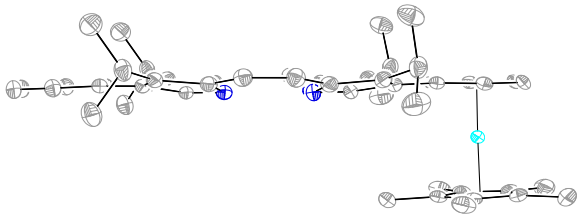

b)

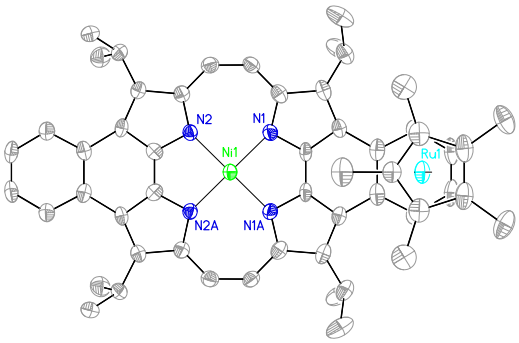

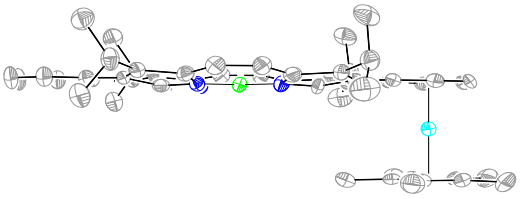

Figure 3.1: a) X-ray crystal structure of **26** (top and side view) showing the atom labeling scheme. Displacement ellipsoids are scaled to the 50% probability level. The complex lies on a crystallographic mirror plane at x, y, ½. Ru lies on the mirror, plane that bisects the macrocycle and the pentamethyl cyclopentadiene moieties. **b)** Top and side view of the bimetallic complex of **27** showing the atom labeling scheme. Displacement ellipsoids are scaled to the 50% probability level. The complex lies on a crystallographic mirror plane of symmetry at z = ½. The mirror plane bisects the porphycene complex and passes through the Ni and Ru ions. Atoms with labels appended by a ‘ are related by x, y, 1-z.

3.2 Spectral Features

The absoption spectra of **24**-**27** revealed a general tendency of broad UV bands at around 265 nm, which are ascribed to the naphthalene moieties of the porphycene. Complexes **24** and **26** were characterized by broad blue-shifted Soret bands, as well as shoulders at higher energy. For instance, the spectrum of complex **24** has energy shoulder on the Soret band. The bimetallic complex **27** and compound **25** displayed less intense Soret bands that were red-shifted compared to those of the metal-free dinaphthoporphycene. However, little shift in the Soret bands was seen in the absorption spectra. This was taken to indicate that coordination of a metallocene to the porphycene core does not significantly change the electronics of the macrocyle as a whole. Complexes with a ruthenocene coordinated to the naphthalene, specifically complexes **24** and **25**, displayed porphycene Q-like bands that were blue-shifted, with Q_{III} and Q_{IV} interchanged in intensities. This was taken as evidence of a significant interaction between the metal and the macrocycle. However, complexes **26** and **27**, displayed a different pattern. Here, the Q_{III} and Q_{IV} bands were found to be red-shifted bands with the relative intensities interchanged (Figure 3.1).

a)

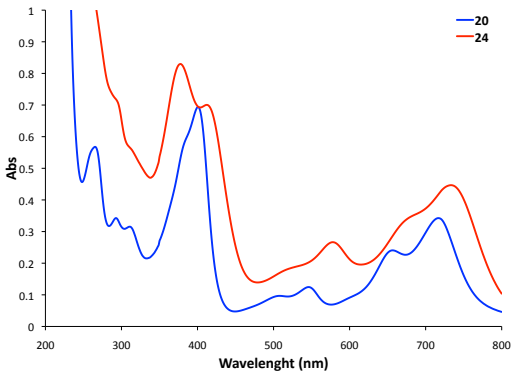

b)

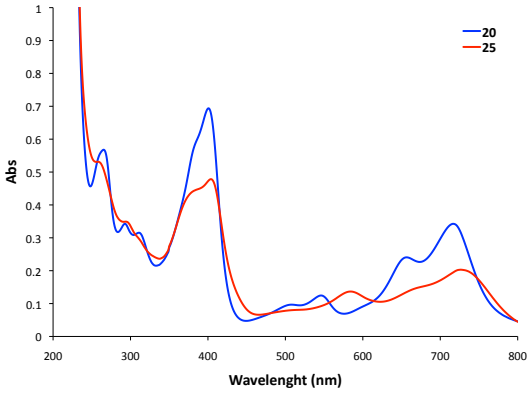

c) d)

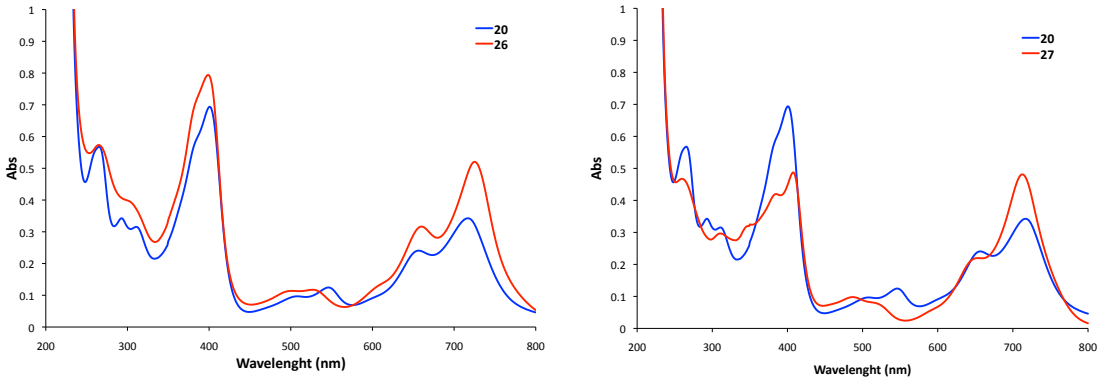

Figure 3.2: a) Absorption spectra of **20** (blue) and **24** (red) in CH_2Cl_2 b) absorption spectra of **20** (blue) and **25** (red) in CH_2Cl_2 c) absorption spectra of **20** (blue) and **26** (red) in CH_2Cl_2 d) absorption spectra of **20** (blue) and **27** (red) in CH_2Cl_2.

3.3 ELECTROCHEMISTRY

The electrochemistry of *i*-propyldinaphthoporphycene, **20**, is characterized by the presence of two well-defined oxidation at and two reduction waves (cf. Table 3.1 and Figure 3.2). Cyclic voltammograms of the metalloporphycenes **21**, **25**, **26**, and **27** were recorded in benzene-acetonitrile mixture, with 0.1 M $TBAPF_6$ as the supporting electrolyte. These analyses revealed the presence of redox waves similar to those of the free macrocycle, **20**, Table 3.1. However, the potential peaks appeared to be broader when the metal is coordinated to the porphycene. The absolute potential separation between these two reductions of the metalloporphycenes varies between 200 and 320 mV.

On the other hand, easier reductions and harder oxidations were observed for all the metallated porphycenes. Particularly, the metalloporphycenes **25** and **26**, that posses a N_4 core free are easier to reduce than the metalloporphycenes that have coordinated nickel(II) cation to the tetraaza central core, **21** and **27** (cf. Table 3.1). For instance, complex **26** is reduced at – 0.55 V in benzene-acetonitrile as compared to complex **27**,

where the electroreduction occurs at – 0.65 V in the same solvent. The lower reduction potential values and the decrease in the electrochemical HUMO-LUMO gap (HLG) of metalloporphycenes with an N_4 core free, indicates a higher electron acceptor character of the *i*-propyldinaphthoporphycene upon the "fusion" of the metallocene on the naphthalene subunit. This is attributed to a loss in symmetry of the porphycene upon the coordination of the metallocene, and the distortion from planarity due steric hindrance that the metallocene produces on the macrocyle. Compound **24** was not studied by electrochemistry due to its limited stability.

	$E_{1/2}$, V vs SCE					
	Ring oxidation		Ring reduction			
Compound	2nd	1st	1st	2nd	HLG	$\Delta E_{1/2}$ (mV)
20	1.27	1.10	-0.65	-0.95	1.75	300
21	-	1.10	-0.60	-0.90	1.70	300
25	-	1.31	-0.28	-0.55	1.59	270
26	1.30	1.00	-0.55	-0.75	1.55	200
27	-	1.00	-0.65	-0.97	1.65	320

Table 3.1: Potentials (V vs SCE) for the oxidation and reduction of investigated *i*-propyldinaphthoporphycene, **20**, and the metalloporphycenes **21**, **25**, **26**, and **27** in benzene-acetonitrile 1:1 (v / v), 0.1 M $TBAPF_6$. Absolute potential difference ($\Delta E_{1/2}$) was calculated between the two reduction peaks. HOMO-LUMO gap (HLG) was calculated between the first reduction potential and the first oxidation potential. All potentials present reversible $E_{1/2}$ values. Peak potentials at 0.1 V/s.

The coordinaion of a ruthenocene to the π-surface of the Ni(II) complex **21** produces a loss of symmetry and a distortion from planarity. These factors affect the electronics of the porphycene. This is evident when the electrochemistry of the hybrid ruthenocene-porphycene system **27** is compared to the Ni(II) complex **21**. Under the same electrochemical conditions the metalloporphycenes displayed one oxidation located at $E_{1/2}$ = 1.00 for **27** and 1.10 V for **21**. Two reductions are also observed at $E_{1/2}$ = – 0.65 and – 0.97 V for **27**, and – 0.60 and – 0.90 V for **21**. The HUMO-LUMO gap of **27** (1.65 V) is lower, when compared with its precursor **21** (1.70 V), Table 3.1. This is attributed

to a significant electronic communication between the organometallic moiety and the electronic core of the macrocyle. This electronic communication produces a photoinduced electron transfer from the rutenocene fragment to the dinapthoporcene core.

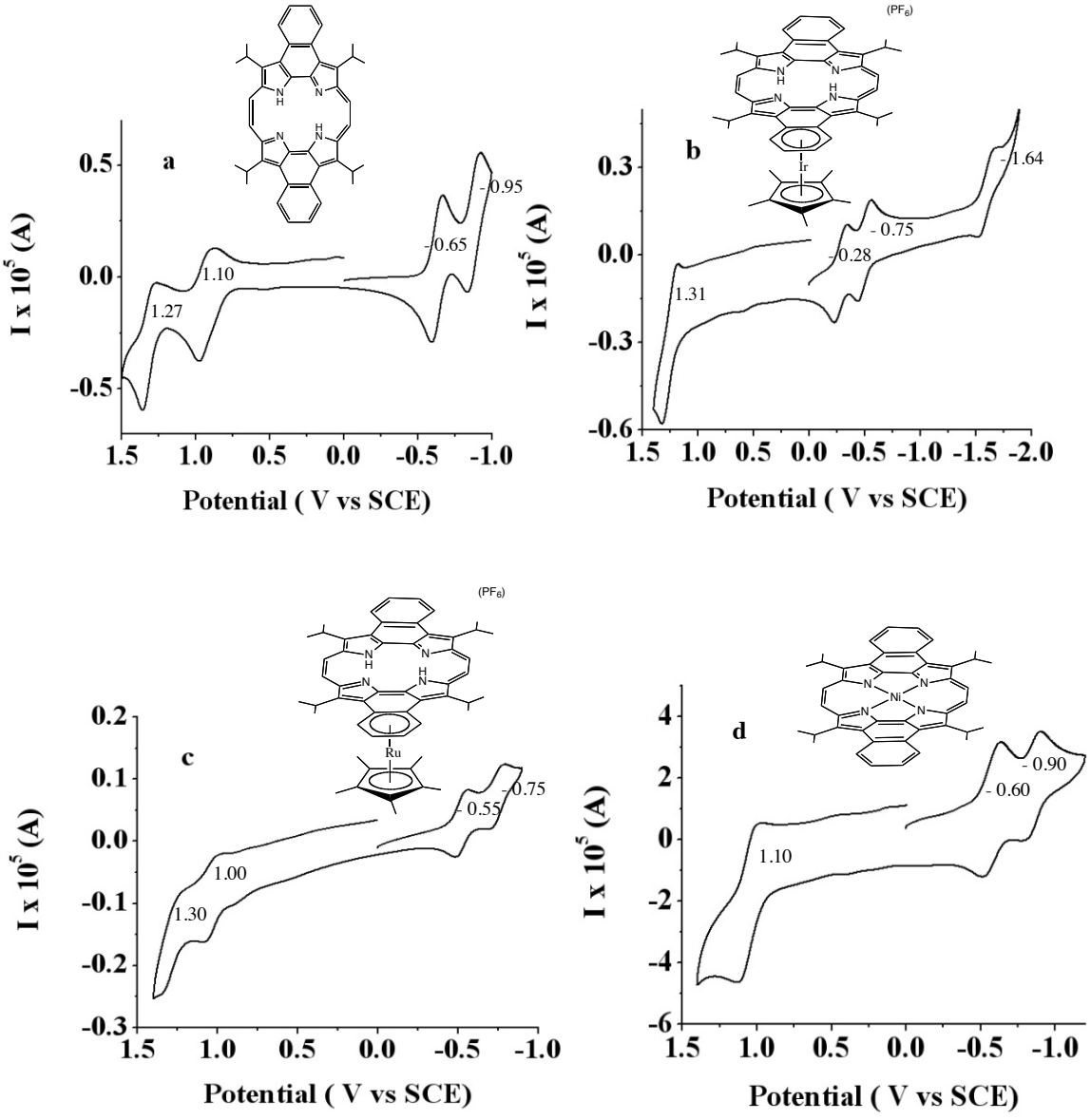

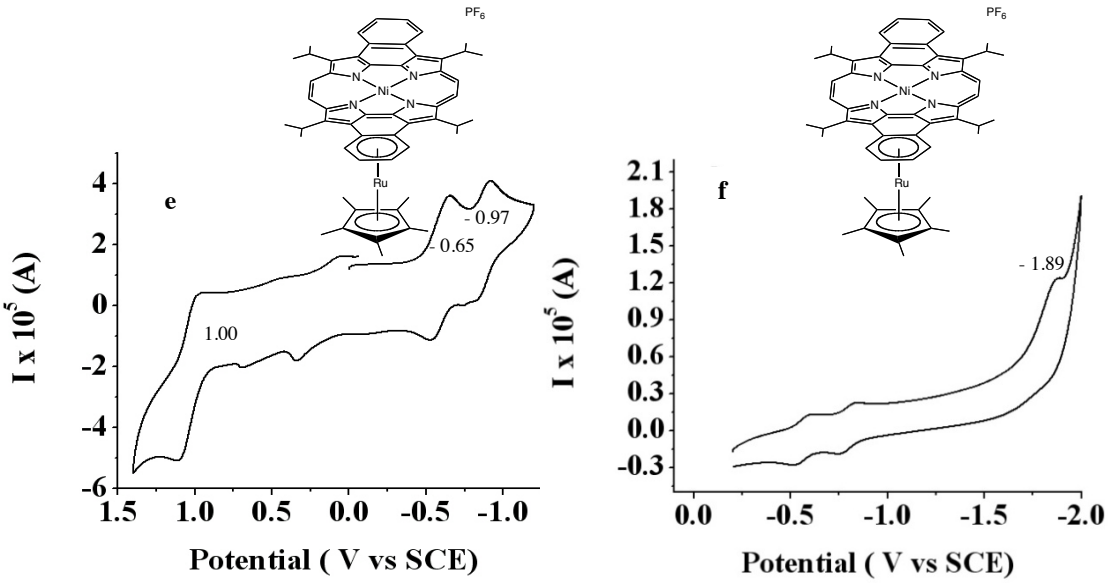

Figure 3.3: Cyclic voltammograms recorded at 295 K for solutions of (a) 0.8 mM porphycene, **20** (b) 0.5 mM Ir complex, **25** (c) 0.15 mM Ru complex, **26**, (d) 5 mM Ni complex, **21** (e) 6 mM Ru-Ni complex, **27** and (f) 0.5 mM Ru-Ni complex, **27**. The solvent used was benzene-acetonitrile 1:1 (v/v) for all samples. The electrodes used were a Pt button (Ø = 0.0314 cm^2) for the working electrode, a Pt wire used as the counter electrode and a saturated calomel electrode employed as a reference electrode (SCE). The supporting electrolyte was $TBAPF_6$, 0.1 M.

3.4 EXPERIMENTAL

3.4.1 General Experimental Procedures

Prior to use, all glassware was soaked in KOH-saturated isopropyl alcohol for ca. 12 h and then rinsed with water and acetone before being thoroughly dried. Dichloromethane and 1,2-dichloroethane were freshly distilled from CaH_2. *o*-Dichlorobenzene was stirred in H_2SO_4 for 24 h, washed with water, dried overnight over $CaCl_2$ and freshly distilled from CaH_2. Free-base *i*-propyldinaphthoporphycene **20**,[29] was prepared following reported procedures. $Ni(acac)_2$ was dried under high vacuum until a crystalline emerald color powder was obtained (ca. 24 h) at 100 °C. $[Ru(Cp^*)(CH_3CN)_3][PF_6]$, $[MCp^*Cl\text{-}(\mu\text{-}Cl)_2]_2$ (M = Rh, Ir) and $AgPF_6$ were purchased

from commercial sources (Strem and Aldrich, respectively) and used as received. All solutions were stirred magnetically. Nuclear magnetic resonance (NMR) spectra were obtained on a Varian Mercury 400 MHz instrument. High-resolution mass spectra were obtained at the University of Texas at Austin, Department of Chemistry and Biochemistry, Mass Spectrometry Facility. Elemental analyses were performed by Atlantic Microlab, Inc., GA.

Electrochemistry. The electrochemical measurements were carried out by Dr. Alexander Nepomnyashchii in the group of Alan J. Bard at the University of Texas at Austin. Tetra-*n*-butylammonium hexafluorophosphate ($TBAPF_6$) was used as the supporting electrolyte and it was recrystallized from ethanol/water (4:1) twice and dried at 100 °C before use. Benzene (Aldrich, anhydrous) and acetonitrile (Aldrich, anhydrous, UV grade) were used as received after being transported unopened into an inert atmosphere drybox (Bosch). Cyclic voltammetry was carried out in a three-electrode cell, which consisted of a platinum button electrode used as working electrode, a platinum counter electrode, and a saturated calomel electrode (SCE) used as a reference electrode. A model 660 electrochemical workstation (CH instruments, Austin, TX) was used for these measurements with a scan rate of 0.1 V/s. A platinum electrode with area of 0.0314 cm^2 was used for all experiments.

Absorption spectra. UV-vis absorption spectra were recorded on a Varian Cary 5000 spectrophotometer. All the spectra were measured in dry CH_2Cl_2, which was purchased commercially and distilled from CaH_2.

3.4.2 Synthesis of Metallodinaphthoporphycene Complexes

The Ni-complex **21** of *i*-propyldinaphthoporphycene was prepared by adding commercially available nickel(II) acetylacetonate to the free base dinaphthoporphycene in *o*-dichlorobenzene in according with the produce reported by Panda *et al*.[36] This

complex was used as a precursor for the synthesis of the hybrid porphycene-ruthenocene compound.

Rh- and Ir-Complex of *i*-Propyldinaphthoporphycene (24 and **25):** $[MCp^*Cl\text{-}(\mu\text{-}Cl)_2]_2$ (M= Rh and Ir; 94 mg, 0.14 mmol, and 80 mg, 0.13 mmol, respectively) was mixed with $AgPF_6$ in dichloromethane (5 mL) at room temperature for 1 h under an argon atmosphere. The suspension obtained was filtered under an inert atmosphere through a pad of celite into a solution of porphycene **20** (15 mg, 0.023 mmol) in 1,2-dichloroethane (10 ml). The reaction mixture was heated at 80 °C for 16 h. After cooling the solvent was evaporated off under reduced pressure. The crude material obtained in this way was purified by column chromatography (neutral alumina 2% MeOH in CH_2Cl_2 eluent). The green or blue-green band was collected and the organic solvent evaporated off under reduced pressure. This gave the products as green solids.

Compound 24: Yield 5.3 mg (33.1%). ^{1}H NMR (400 MHz, 296 K, $CDCl_3$): δ (ppm) 9.67 (s, 2H, *meso*-CH), 9.49 (s, 2H, *meso*-CH), 8.66 (m, 2H, CH-naphthalene), 7.59 (m, 4H, CH-naphthalene), 4.76 (m, 2H, CH-alkyl), 4.62 (m, 2H, CH-alkyl), 2.28 (m, 12H, CH-alkyl), 1.76 (d, (J = 5.9 Hz), 6H, CH-alkyl), -0.19 (s, 15H, C_5Me_5). ^{13}C NMR (100.6 MHz, 296 K, $CDCl_3$): δ (ppm) 149.4, 142.9, 141.1, 137.8, 136.4, 133.8, 132.1, 131.0, 127.1, 128.0, 117.2, 116.4, 103.9, 87.6 28.7, 27.5, 27.6, 25.3, 23.7, 8.1. HR-ESI (m/z): 863.3638 (calc. For $[C_{54}H_{56}N_4Rh]^{+1}$: 863.3559).

Compound 25: Yield 6.1 mg (43.6%). ^{1}H NMR (400 MHz, 296 K, $CDCl_3$): δ (ppm) 9.68 (br, 2H, *meso*-CH), 9.48 (br, 2H, *meso*-CH), 8.67 (m, 2H, CH-naphthalene), 8.61 (m, 2H, CH-naphthalene), 7.62 (m, 4H, CH-naphthalene), 4.55 (br, 2H, CH-alkyl), 4.51 (br, 2H, CH-alkyl), 2.30 (m, 12H, CH-alkyl), 1.71 (m, 12H, CH-alkyl), -0.135 (s, 15H, C_5Me_5). ^{13}C NMR (100.6 MHz, 296 K, $CDCl_3$): δ (ppm) 148.4, 144.4, 141.1, 138.7, 136.4, 133.8, 132.2, 131.2, 128.1 128.2, 117.7, 116.2, 105.0, 88.7 29.7, 27.9, 27.9, 25.4, 23.6, 8.1. HR-ESI (m/z): 953.4212 (calc. For $[C_{54}H_{56}N_4Ir]^{+1}$: 953.4119). Anal. Calc. for $C_{55}H_{61}N_4OIrPF_6$ (**27**·CH_3OH): C, 58.39; H, 5.43; N, 4.95. Found: C, 58.82; H, 5.46; N, 4.95.

Ru-Complex of *i*-Propyldinaphthoporphycene (26): To a solution of **20** (12 mg, 0.019 mmol) in dry dichloromethane (10 mL) was added $[RuCp^*(NCMe)_3]PF_6$ (58 mg, 0.115 mmol). The reaction mixture was then stirred under an argon atmosphere for 4 h. The solvent was reduced in volume under reduced pressure until a volume of 2 mL remained. The resultant product was purified using a neutral alumina column and 1% MeOH in CH_2Cl_2 as eluent. The green-blue fraction was collected and the organic solvent evaporated to give a dark blue solid that was recrystallized from the mixture CH_2Cl_2/diethylether. Yield: 7 mg (40.9%). ^{1}H NMR (400 MHz, 296 K, CD_2Cl_2): δ (ppm) 9.66, 9.53 (d (*J* = 2.8 Hz), 2H, *meso*-CH), 9.51, 9.522 (d (*J* = 5.7 Hz), 2H, *meso*-CH), 9.26 (s, 2H, N-H), 8.68-8.66 (m, 2H, CH-naphthalene), 7.60-7.58 (m, 2H, CH-naphthalene), 7.09-7.07 (m, 2H, CH-naphthalene), 6.29-6.27 (m, 2H, CH-naphthalene), 4.81 (m, 2H, CH-alkyl), 4.52 (m, 2H, CH-alkyl), 2.21 (m, 12H, CH-alkyl), 2.02 (dd (*J*= 1.8 Hz, 6.7 Hz), 12H, CH-alkyl), 1.35 (s, 15H C_5Me_5). ^{13}C NMR (100.6 MHz, 296 K, CD_2Cl_2): δ (ppm) 146.5, 146.8, 145.1, 133.0, 131.8, 130.4, 127.8, 128.0, 125.3, 117.9, 116.7, 96.4, 95.8, 87.7, 84.7, 29.7, 28.3, 28.4, 25.7, 24.4, 9.3. HR-ESI (m/z): 863.36286 (calc. For $[C_{54}H_{57}N_4Ru]^{+1}$: 863.3621). Anal. Calc. for $C_{54}H_{57}N_4RuPF_6$: C, 64.34; H, 5.70; N, 5.56. Found: C, 64.49; H, 6.09; N, 5.17. This complex was also characterized by single crystal X-ray diffraction analysis.

Hybrid Porphycene-Ruthenocene System (27): An excess of $[Ru(Cp^*)(CH_3CN)_3][PF_6]$ (30 mg, 0.060 mmol) was added to a solution of the corresponding Ni(II)-porphycene **21** (10 mg, 0.014 mmol) in dry CH_2Cl_2 (10 mL). The reaction mixture was heated at reflux for 12 h under an argon atmosphere. After cooling, the solvent was reduced under low pressure until a volume of 2 mL remained. The resulting solution was then purified by preparatory thin layer chromatography (alumina, 2% MeOH in CH_2Cl_2, eluent). The desired product band was identified by its green color. The band was removed and suspended in CH_2Cl_2. The suspension was filtered through a pad of celite and the organic solvent removed under vacuum. The resulting product was recrystallized from a mixture

MeOH-CH_2Cl_2/diethylether to yield 4.5 mg (24.7%) of the product **27**. ^{1}H NMR (400 MHz, 296 K, CD_2Cl_2): δ (ppm) 9.27 (d, (*J* = 2.9 Hz), 2H, *meso*-CH), 9.11 (d, (*J* = 2.8 Hz), 2H, *meso*-CH), 8.49 (m, 2H, CH-naphthalene), 7.52 (m, 2H, CH-naphthalene), 4.60 (br, 2H, CH-alkyl), 4.51 (br, 2H, CH-alkyl), 2.24 (m, 12H, CH-alkyl), 1.97 (m, 12H, CH-alkyl), 0.07 (s, 15H, C_5Me_5). ^{13}C NMR (100.6 MHz, 296 K, CD_2Cl_2): δ (ppm) 147.5, 147.8, 145.2, 134.7, 130.4, 130.1, 128.0, 128.2, 125.5, 118.7, 117.1, 96.6, 96.0, 87.6, 84.7, 29.9, 28.1, 28.3, 26.0, 24.4, 9.3. HR-ESI (m/z): 919.2833 (calc. For $[C_{54}H_{55}N_4NiRu]^{+1}$: 919.2824). This complex was also characterized by single crystal X-ray diffraction analysis.

Bibliography

(1) J. Waluck, M. Muller, P. Swiderek, M. Kocher, E. Vogel, G. Hohlneicher, J. Michi, *J. Am. Chem. Soc.* **1991**, *113*, 5511-5527.

(2) K. M. Kadish, E. Van Caemelbecke, P. Boulas, F. D'Souza, E. Vogel, M. Kisters, C. J. Medforth, K. M. Smith, *Inorg. Chem.* **1993**, *32*, 4177-4178.

(3) E. Vogel, *J. Heterocycl. Chem.* **1996**, *33*, 1461-1487.

(4) A. Starukhim, E. Vogel, J. Waluk, *J. Phys. Chem. A* **1998**, *102*, 9999-10006.

(5) E. Steiner, P. W. Fowler, *Org. Biomol. Chem.* **2003**, *1*, 1785-1789.

(6) A. Vdovin, J. Sepiol, N. Urbanska, M. Pietraszkicwicz, A. Mordzinski, J. Waluk, *J. Am. Chem. Soc.* **2006**, *128*, 2577-2586.

(7) J. Waluk, *Acc. Chem. Res.* **2006**, *39*, 945-952.

(8) K. Aoki, T. Goshima, Y. Kozuka, Y. Kawamori, N. Ono, Y. Hisaeda, H. D. Takayi, M. Inamo, *Dalton Transactions* **2009**, 119-125.

(9) J. Arnbjerg, J.-B. Ana, J. P. Martin, S. Nonell, J. L. Borrell, O. Christiansen, P. R. Ogilby, *J. Am. Chem. Soc.* **2007**, *129*, 5188-5199.

(10) L. R. Milgrom, *The Colours of Life: An Introduction to the Chemistry of Porphyrins and Related Compounds*, Oxford University Press, Oxford, **1997**.

(11) *The Porphyrin Handbook: Synthesis and Organic Chemistry*, Vol. 6, Academic Press, San Diego, **2000**, pp. 157-168, 196-198.

(12) E. Vogel, M. Köcher, H. Schmickler, J. Lex, *Angew. Chem. Int. Ed. Engl.* **1986**, *25*, 257-259.

(13) M. Grosmann, B. Franck, *Angew. Chem. Int. Ed. Engl.* **1986**, *25*, 1100-1101.

(14) D. Sánchez-García, J. L. Sessler, *Chem. Soc. Rev.* **2008**, *37*, 215-232.

(15) F. D'Souza, P. Boulas, A. M. Aukauloo, R. Guilard, M. Kisters, E. Vogel, K. M. Kadish, *J. Phys. Chem.* **1994…**

(16) Z.-Y. Li, J.-S. Huamg, C.-M. Che, C. K. Chang, *Inorg. Chem.* **1992**, *31*, 2670-2672.

(17) C.-M. Che, C.-K. Poon, W.-C. Chung, H. B. Gray, *Inorg. Chem.* **1995**, *24*, 1277-1278.

(18) C.-M. Che, W.-C. Chung, T.-F. Lai, *Inorg. Chem.* **1988**, *27*, 2801-2804.

(19) C.-M. Che, W.-H. Leung, W.-C. Chung, *Inorg. Chem.* **1990**, *29*, 1841-1846.

(20) N. J. Gogan, Z. U. Siddiqui, *J. Chem. Soc. D* **1970**, 284-285.

(21) N. J. Gogan, Z. U. Siddiqui, *Can. J. Chem.* **1972**, 50, 720-725.

(22) H. J. H. Wang, L. Jaquinod, D. J. Nurco, M. Graca, H. Vicente, K. Smith, *Chem. Commun.* **2001**, 2646-2647.

(23) H. J. H. Wang, L. Jaquinod, D. J. Nurco, M. M. Olmstead, M. Graca, H. Vicente, K. M. Kadish, Z. Ou, K. Smith, *Inorg. Chem.* **2007**, *46*, 2898-2913.

(24) K. K. Dailey, G. P. A. Yap, A. L. Rheingold, T. B. Rauchfuss, *Angew. Chem. Int. Ed. Engl.* **1996**, *35*, 1833-1835.

(25) K. K. Dailey, T. B. Rauchfuss, *Polyhedron.* **1997**, *16*, 3129-3128.

(26) L. Cuesta, E. Karnas, V. M. Lynch, J. L. Sessler, W. Kajonkijya, W. Zhu, M. Zhang, Z. Ou, K. M. Kadish, K. Ohkubo, S. Fukuzumi, *Chem.-Eur. J.* **2008**, *14*, 10206-10210.

(27) L. Cuesta, J. L. Sessler, *Chem. Soc. Rev.* **2009**, *38*, 2716-2729.

(28) L. Cuesta, S. Fukuzumi, J. L Sessler, *J. Am. Chem. Soc.* **2009**, *131*, 13538-13547.

(29) V. Roznyatovskiy, V. M. Lynch, J. L. Sessler, *Org. Lett.* **2010**, *12*, 4424-4427.

(30) J. L. Sessler, S. J. Weghorn, *Expanded, Contracted and Isomeric Porphyrins*, Pergamon, Elmsford, N. Y. **1997**, pp. 127-423.

(31) O. S. Finikova, S. E. Aleshchenkov, R. P. Brinas, A. V. Cheprakov, P. J. Carroll, S. A. Vinogradov, *J. Org. Chem.* **2005**, *70*, 4617-4628.

(32) E. Vogel, *Pure Appl. Chem.* **1993**, *65*, 143-152.

(33) J. Dockowski, V. Galievsky, A. Starukhin, E. Vogel, J. Waluk, *J. Phys. Chem, A.* **1998**, *102*, 4966-4971.

(34) J. Dobkowski, Y. Lobko, S. Gawinski, J. Waluk, *J. Chem. Phys. Lett.* **2005**, *416*, 128.

(35) D. Kuzuhana, J. Mack, H. Yamada, T. Okujima, N. Ono, N. Kobayashi, *Chem.-Eur. J.* **2009**,*15*, 10060-10069.

(36) T. Sarma, P. K. Panda, P. T. Anusha, S. V. Rao, *Org. Lett.* **2011**, *13*, 188-191.